Assembly of Synthetic Functional Cellulosomal Structures onto the Cell Surface of Lactobacillus plantarum, a Potent Member of the Gut Microbiome

Assembly of synthetic functional cellulosomal structures onto the *Lactobacillus plantarum* cell surface – a potent member of the gut microbiome

Johanna Stern[a*], Sarah Moraïs[a, b*], Yonit Ben-David[a], Rachel Salama[c], Melina Shamshoum[a], Raphael Lamed[d], Yuval Shoham[c], Edward A Bayer[a] and Itzhak Mizrahi[b†]

[a]*Department of Biomolecular Sciences, The Weizmann Institute of Science, Rehovot 7610001 Israel;*

[b]*Faculty of Natural Sciences, Ben-Gurion University of the Negev, Beer-Sheva 8499000 Israel*

[c]*Department of Biotechnology and Food Engineering The Technion Israel Institute of Technology, Haifa 32000 Israel;*

[d]*Department of Molecular Microbiology and Biotechnology, Tel Aviv University, Ramat Aviv 69978 Israel*

[*]J.S. and S.M. contributed equally to this work.

†To whom correspondence should be addressed:

Itzhak Mizrahi

Tel: (+972)- 8 647 79 859

Email: imizrahi@bgu.ac.il

Running title: Extended cell surface assembly of fibrolytic complex

Abstract

Heterologous display of enzymes on microbial cell surfaces is an extremely desirable approach, since it enables the engineered microbe to interact directly with the plant-wall extracellular polysaccharide matrix. In recent years, attempts have been made to endow non-cellulolytic microbes with genetically engineered cellulolytic capabilities for improved hydrolysis of lignocellulosic biomass and for advanced probiotics. Thus far, however, owing to the hurdles of secreting and assembling large, intricate complexes on the bacterial cell wall, only free cellulases or relatively simple cellulosome assemblies have been introduced into live bacteria. Here, we employed the "adaptor scaffoldin" strategy to overcome the low levels of protein displayed on the bacterial cell surface. The approach mimics natural cellulosome elaborated architectures, thus exploiting the exponential features of their Lego-like combinatorics. Using this approach, we produced several bacterial consortia of *Lactobacillus plantarum*, a potent gut microbe which provides a very robust genetic framework for lignocellulosic degradation. We successfully engineered surface display of large, fully active self-assembling cellulosomal complexes containing an unprecedented number of catalytic subunits all produced *in vivo* by the cell-consortia. Our results demonstrate superior enzyme stability and performance of the cellulosomal machinery, compared to the equivalent secreted free enzyme system and high cellulase-to-xylanase ratios proved beneficial for efficient degradation of wheat straw.

Importance

48 The multiple benefits of lactic acid bacteria are well established in health and industry.
49 Here we present an approach to extensively increase the cell-surface display of proteins
50 via successive assembly of interactive components. Our findings present a stepping stone
51 towards proficient engineering of *Lactobacillus plantarum*, a widespread,
52 environmentally important bacterium and potent microbiome member, for improved
53 degradation of lignocellulosic biomass and advanced probiotics.
54

Introduction

The plant cell wall is a tough and rigid layer that surrounds the cell to withstand internal osmotic pressure resulting from the difference in solute concentration between the cell interior and external water (1). It is composed of various polysaccharides (mostly cellulose and hemicellulose) and the crosslinked, phenolic polymer lignin. Degradation of the plant cell wall is performed in nature by various microbial systems that have evolved in order to utilize its sugars as a main carbon source. The cellulosome (2), first characterized in the thermophilic anaerobe *Clostridium thermocellum* (3), is a large, highly cellulolytic multi-enzymatic complex that can be either anchored to the bacterial cell surface (4, 5) or secreted to the extracellular medium. Cellulosomal complex formation is based on a unique type of intermodular interaction between its components: the enzymes and the scaffoldins. Multiple cohesin modules on the scaffoldin and individual dockerin modules on the enzyme subunits interact in a noncovalent manner with very high affinity that approaches and surpasses that of antigen-antibody binding (6). The close proximity between the multiple enzymes serves to enhance synergistic activity (7), and the carbohydrate-binding module (CBM), usually contained in the scaffoldin subunit, targets the entire complex to the substrate. When anchored to the bacterial surface, the cellulosome also contributes to minimal diffusion loss of enzymes and degradation products.

In the past, several studies have reported the fabrication of artificial, chimaeric, cellulosomal structures, engineered for displayed on the surfaces of various microbial

77 strains, notably *Saccharomyces cerevisiae* (8–11), *Bacillus subtilis* (12, 13), *Clostridium*
78 *acetobutylicum* (14) and *Lactococcus lactis* (15). For this purpose, designer cellulosome
79 technology has been employed to mimic the architecture of cellulosome complexes
80 and/or specifically control their enzyme composition (16–19). One of the major issues of
81 cell-surface attachment of chimaeric scaffoldins is the low level of surface display that
82 leads to slow catalysis and low fermentation efficiency (10, 20). The feasibility of
83 transferring cellulosomal technologies to a bacterium with potential industrial and clinical
84 applications has been demonstrated recently in *Lactobacillus plantarum* (21–23).
85 Although this bacterium lacks the native capacity both to degrade cellulosic substrates
86 and to produce biofuels like ethanol, it is highly tolerant to low pH and ethanol (up to 13%
87 (v/v)) (24) and has been identified as a main contaminant in biofuel refineries (25).
88 Therefore, it could also represent an attractive candidate vehicle for consolidated
89 bioprocessing (CBP) (21, 22). *L. plantarum* is also a member of the human gut microbiome
90 (26) and additional gut ecosystems (27) and affects host attributes such as mate selection
91 and growth (28, 29). Moreover, strains belonging to this species were recently shown to
92 promote juvenile growth and buffer the effect of chronic undernutrition in germ-free
93 mice (30).

94 Previously, the lignocellulolytic capabilities of engineered *L. plantarum* towards
95 simple polysaccharides and wheat straw were demonstrated by introducing two key
96 enzymes, a cellulase and a xylanase, from the thermophilic bacterium *Thermobifida fusca,*
97 using the previously developed pSIP vectors (31) for efficient secretion of heterologous
98 proteins (21, 22). The two enzymes were also shown to be displayed directly on the cell

surface of cellulosomes, by which the assembly of the enzymes onto a chimaeric scaffoldin was controlled by specific cohesin-dockerin interactions. The secreted enzymes were the most active of the three strategies at early times of degradation; but, as component parts of the surface-attached designer cellulosomes, the enzymes were more stable in time and achieved similar levels of degradation compared to those of the secreted enzymes during later times of degradation. In these latter studies, we devised a novel cell consortium approach in which each engineered *L. plantarum* strain expressed and secreted different components of the complex to be assembled on the cell wall of a scaffoldin-expressing strain (21, 22). The labor of producing and secreting the cellulosomal components was therefore divided among the bacterial community.

Nevertheless, due to hurdles of anchoring large scaffoldins on the *L. plantarum* cell-wall, we were limited in assembling only small numbers of enzymes in the cellulosomal complex, thus restricting the fiber-degradation capabilities of the engineered cell consortium. In order to reach superior levels of degradation of the recalcitrant fiber, and to exploit the potential of the cellulosomal complex, more enzymatic functions have to be incorporated into the cellulosomal machinery. In order to overcome these issues, we have, in the current work, mimicked naturally existing molecular tactics to amplify the inherent enzyme combinatorics and stoichiometric plasticity used by several cellulosome-producing bacteria (32, 33). This approach allows the expression of large, stable and active self-assembling protein complexes on the bacterial cells and may provide an effective strategy to achieve enhanced cell-surface display of the engineered enzymes thereby expanding the lignocellulolytic potential in *L.*

plantarum.

Results

Engineering of fully active mesophilic enzymes for assembly of cellulosomal structures on the *L. plantarum* cell wall. Since the host 'vehicle' for our study, *L. plantarum,* is a mesophile, we searched for appropriate enzymes derived from mesophilic bacteria to be used as designer cellulosome components for surface display. Our recent involvement in genomic sequencing of the mesophilic cellulolytic bacterium, *C. papyrosolvens* (34), provided a wealth of potentially compatible enzymes for our study.

The *C. papyrosolvens* enzymes, selected for heterologous secretion in *L. plantarum* destined for self-assembly into active designer cellulosomes on the *L. plantarum* cell surface, are shown schematically in Fig. 1A. *C. papyrosolvens* exhibits strong genome homology with the closely related mesophile, *Clostridium cellulolyticum*, which was demonstrated previously to possess highly efficient polysaccharide-degrading enzymes, both in the context of *in vitro* designer cellulosomes (17, 35) and for yeast- or bacterial-based CBP (14, 36). Two putative *C. papyrosolvens* cellulases, GH5 and GH9, were selected on the basis of their homology with the two known synergistic cellulases from *C. cellulolyticum,* i.e., the processive endoglucanase Cel9G and the Cel5A endoglucanase (17). Two putative xylanases were also selected: one from the GH11 family, homologous to *C. cellulolyticum* Xyn11A, and another from the GH10 family, homologous to *C. cellulolyticum* Xyn10A. Both of the *C. cellulolyticum* enzymes were characterized as efficient xylanases (37, 38).

The cohesin-dockerin assembly is species-specific (39, 40). Therefore, in order to

control the composition and architecture of the desired designer cellulosomes, each enzyme was designed to contain a dockerin derived from a distinct bacterial species that will match a specific cohesin on the chimaeric scaffoldin (16). The chimaeric enzymes were thus modified by replacing the original *C. papyrosolvens* dockerin module (that share the same binding specificity) with dockerins from other bacterial species, resulting in enzymes with different cohesin-binding specificities.

The hydrolytic activity of each of the five purified recombinant chimaeric enzymes from *C. papyrosolvens* was compared to that of the corresponding recombinant wild-type enzyme, all produced in *Escherichia coli* (Supplementary materials: Fig. S1). The wild-type enzymes and their respective recombinant chimaeras were fully active on all cellulosic substrates or on xylan.

Newly designed recombinant synthetic scaffoldins. In order to increase the combinatorics of the synthetic cellulosomal machinery, we have mimicked the existing natural microbial "adaptor-scaffoldin" approach into heterogeneous bacterial cells (36, 41, 42). In this approach, several scaffoldins are assembled together through mediation via adaptor scaffoldin(s) thereby increasing the number of enzymatic components in the cellulosomal complex (Fig. 1D). We designed two types of adaptor scaffoldins for enzyme integration (Fig. 1B): one type, Adaptor·1, contains the two cohesin modules that bind the two dockerin-containing cellulases, and the second, Adaptor·2, contains two cohesin modules that incorporate the two dockerin-containing xylanases. In addition to the 2 enzyme-integrating cohesins, each adaptor scaffoldin contains a substrate-targeting CBM

and a type II or type III dockerin, respectively, for interaction with the cell surface-anchoring scaffoldin (42).

As mentioned above, one of the advantages of using the adaptor-scaffoldin approach is that it amplifies the combinatoric and stoichiometric possibilities for enzyme integration. In order to explore the combinatorical possibilities and to increment methodically the number of enzymes integrated into the complex, we created 5 different types of anchoring scaffoldins, as represented in Fig. 1C, that enable the insertion of up to 8 enzymes into the displayed designer cellulosomes. All of the anchoring scaffoldins contain a sortase signal motif for covalent attachment to the cell-surface via a resident *L. plantarum* sortase (43). While Anc·1 is composed of four different type I cohesin modules that directly interact with the four dockerin-bearing enzymes (the two cellulases and the two xylanases); Anc·2, Anc·3 and Anc·4 possess several copies of type II and III cohesins with different specificities. This setup of divergent specificities also allows us to analyze the influence of stoichiometry of the xylanases versus the cellulases on plant fiber degradation by enabling the attachment of either one or two copies of the cellulase-bearing adaptor scaffoldin (Adaptor·1) or one or two copies of the xylanase-bearing adaptor scaffoldin (Adaptor·2). An example of the various cell-surface-displayed cellulosome assemblies produced by the different cell consortia is shown in Fig. 1D.

In order to examine the binding abilities of our engineered complexes, the two adaptor scaffoldins and five anchoring scaffoldins were initially purified recombinantly in *E. coli*. The respective binding specificities of the cohesin and dockerin modules of both the purified adaptor scaffoldins and anchoring scaffoldins were examined by performing

native gel electrophoresis, and each recombinant protein was shown to interact selectively with its expected partner (see example in Fig. S2).

Secretion of active recombinant *C. papyrosolvens* mesophilic enzymes by *L. plantarum*

The secretion and functionality of enzymes by *L. plantarum* were analyzed by comparing the enzymatic activity of concentrated culture supernatant fluids from transformed lactobacilli with that of the pure recombinant proteins from *E. coli* (Fig. S3). The two xylanases actively degraded xylan, and their concentration was thus estimated (Fig. S3A and B, Table 1). The two cellulases were not properly secreted using leader peptide Lp3050 (data not shown). We therefore selected an alternative leader peptide (Lp2588), which was also reported as an efficient candidate for secretion of foreign proteins in *L. plantarum* (31). The cellulase activities observed in Figs. S3C and D served to estimate the concentrations of the respective proteins (Table 1) (21). In parallel, we verified the presence of full-length recombinant enzymes and their ability to properly bind their respective cohesin modules by Far Western blot analysis (Supplementary materials: Fig. S4).

***L. plantarum* secretes and anchors active chimaeric scaffoldins** After examining the proper functionality and integrity of the enzymes to function within the cellulosomal complex, we examined the expression of anchoring and adaptor scaffoldins in *L. plantarum,* which will integrate the enzymes to form the desired elaborate cellulosomal structures.

The secretion of the adaptor scaffoldins and their functionality were analyzed using an ELISA-based binding assay by comparing the binding properties of the pure recombinant proteins (produced in *E. coli*) to culture supernatants from transformed lactobacilli. We found that the adaptor scaffoldins were properly secreted into the extracellular medium and exhibited the expected cohesin-dockerin binding capacities (Supplementary materials Fig. S5). In addition, in Fig. 2 we can observe that the binding properties of the adaptor scaffodins attached to the anchoring scaffoldins are functional. The presence of full-length adaptor scaffoldins was also verified by Western blot analysis (Supplementary materials Fig. S4). The anchoring and functionality of the chimaeric scaffoldins were also analyzed by ELISA-based binding assay by comparing the binding properties of pure proteins (xylanase tag fused to the different dockerins) to washed whole bacterial cells from transformed lactobacilli (Supplementary materials Fig. S6). We observed that anchoring scaffoldins composed of two and three cohesins (Anc·2, Anc·3a and Anc·3b) were attached and fully functional on the *L. plantarum* cell surface. Both cohesin/dockerin pairs, appeared to enable comparably high interaction events (Supplementary materials Fig. S6). On the other hand, anchoring scaffoldins composed of 4 cohesins (Anc·1 and Anc·4) did not exhibit full binding abilities, as they showed insufficient binding for two of their cohesins (Fig. 2 and Supplementary materials Fig. S6). In both cases, the cohesins adjacent to the anchoring signal motif were not functional. This result emphasizes the importance of using the adaptor scaffoldin strategy in this system, since incorporation of four different dockerin-bearing enzymes extends the number of catalytic subunits, and this would not be achieved by using a single scaffoldin

directly anchored onto the *L. plantarum* cell surface.

ELISA-based binding assays both for adaptor and anchoring scaffoldins also served to evaluate the quantity of secreted or anchored proteins of the different transformed strains of *L. plantarum* by using standard curves of known concentrations of pure proteins (Table 1).

***L. plantarum* cells displaying synthetic elaborate cellulosomal machinery show superior performance over secreted enzymes and simple synthetic cellulosome strategies.** As we reported previously (22), the cell consortia approach is a highly efficient way for assembling large complexes on bacterial cell walls. In this approach, the effort of producing and secreting the cellulosomal complex is divided among several strains – each secreting a different cellulosomal component of the cellulosome, thereby enabling its combined assembly on the cell wall of the anchored scaffoldin-containing strain. In addition, since we obtained relatively large differences in the quantity of secreted/anchored proteins, the flexibility provided by the cell consortium approach is essential to control the production of cellulosomal complexes, which stoichiometric amounts of the relevant components.

Here, we examined the ability of the elaborate cellulosomal machineries to degrade natural plant fiber material (pre-treated wheat straw) as well as to compare their action to that of the free secreted enzyme approach. To this end, six different types of microbial consortia were examined as detailed in Fig. 3B. Using these consortia, we experimented with different stoichiometries of the cellulosomal and secreted enzyme components (Fig.

253 3A).

254 Microbial consortia examined in this work produce either the free enzymes or the
255 surface-displayed designer cellulosomes, and the bacterial cells would directly consume
256 the sugars produced by their different enzymatic arrangements. Hence, in order to
257 elucidate the portion of sugars that is consumed by our microbial consortia we performed
258 *in vitro* enzymatic hydrolysis with enzymes or assembled designer cellulosomes produced
259 and purified from *E. coli* (Fig. 3C), in order to determine the level of soluble sugar
260 production in the absence of *L. plantarum* cells. Indeed, as presented in Fig. 3C, we
261 observed higher amounts of sugars produced by the enzymatic mixtures as opposed to
262 the residual sugars measured after incubation with the microbial consortia (Fig. 3A). In
263 addition, we could see from both Figs. 3A and C that the designer cellulosomes
264 consistently outperformed their respective free enzyme counterparts (bars 1, 2 and 3
265 compared to 4, 5 and 6).

266 In Fig. 3C, the comparative degradation of pre-treated wheat straw by the *in vitro*-
267 applied enzymes and designer cellulosomes revealed that designer cellulosomes
268 comprising two copies of the cellulases (bar 2) was the best-performing enzymatic
269 complex. By comparison, in Fig. 3A, the soluble (residual) sugar measurements reflected
270 the amount of sugars that were not consumed by the *L. plantarum* consortia. We then
271 further evaluated the kinetics of the reaction were also evaluated using microbial
272 consortia, which revealed the continued activity of the anchored designer cellulosomes
273 until 96 h, whereas the free enzymes failed to produce additional soluble sugars after 48h
274 (Fig. S7). Further analysis of unconsumed released sugars from pre-treated wheat straw

degradation using high performance anionic exchange chromatographic (Table S1), revealed high amounts of xylan degradation products (mainly xylobiose and xylotriose), suggesting that *L. plantarum* could not assimilate these carbon sources.

Discussion

In this study, we used the adaptor scaffoldin strategy for assembly of elaborate cellulosomal structures (36, 41, 42) on the cell surface of *L. plantarum* for both augmenting cell-surface display and improving its fiber-degrading potential. For this purpose, the use of potent enzymes originating from a mesophilic cellulosome-producing species, *Clostridium papyrosolvens*, is well-suited for expression in the gut ecosystem (a common *L. plantarum* habitat). Here, all the cellulosomal components were produced *in vivo* by the cell-consortia and not supplemented *ex vivo* as previously reported (36, 41).

Cellulosomal complexes have attracted increased interest in recent years, since lignocellulosic biomass represents a particularly abundant resource for conversion into fermentable sugars, suitable for production of biofuels (44). We recently reported the successful incorporation of simple divalent designer cellulosome components onto the cell wall of *Lactobacillus plantarum* (22), an attractive candidate for consolidated bioprocessing (22, 45, 46). Here, the adaptor scaffoldin strategy was demonstrated to be an effective approach (i) for increasing the number of catalytic units in the cellulosome complex displayed on the cell-surface, thereby bypassing the relatively low cell-surface display of scaffoldins, and (ii) for achieving high binding capacities of the bacterial cell to the substrate.

297 In this work, we produced elaborate cellulosomal complexes by employing a cell-
298 consortium approach, whereby each recombinant strain of *L. plantarum* expresses an
299 individual cellulosomal component (secreted to the extracellular medium or anchored to
300 the bacterial cell surface). A total of four chimaeric cellulosomal enzymes (cellulases and
301 xylanases derived from *C. papyrosolvens*) and two adaptor scaffoldins were functionally
302 secreted into the extracellular media. In addition, five different types of anchoring
303 scaffoldins were tested for their ability to properly interact subsequently with the
304 secreted cellulosomal elements. By composing various co-cultures of recombinant
305 bacteria expressing the heterologous proteins separately, we were able to attach up to
306 three adaptor scaffoldins to the anchoring scaffoldins for potential display of up to six
307 catalytic subunits on the cell surface. Using co-cultures offers the advantage that the
308 composition of the surface-anchored designer cellulosome, produced by an appropriate
309 cell consortium, can be easily controlled by adjusting the ratio of each cell type during
310 inoculation. It was also demonstrated that co-cultures of recombinant bacteria expressing
311 heterologous proteins did not affect the initial ratio of the strains and therefore did not
312 affect the ratio of proteins expressed (21). The cell-consortium approach decreases
313 considerably the burden of the cellular machinery of each strain, thereby maximizing their
314 ability to grow and to express the various cellulosomal components. In nature, this type
315 of spatial differentiation strategy is commonly employed by prokaryotic species in a given
316 ecosystem, which results in a collaboration among the different cell types to achieve a
317 unique objective from which they will all benefit (47).
318 The variety of anchoring and adaptor scaffoldins allowed us to examine the

importance of ratios among the different enzymatic components in order to obtain efficient substrate degradation. The highest levels of degradation in the present studies were obtained when a trivalent anchoring scaffoldin enabled attachment to the cell surface of three adaptor scaffoldins incorporating a total of four cellulases (2 copies of Adaptor 1) and two xylanases (single copy of Adaptor 2) (see Fig. 3C, Bar 2). This enzymatic combination was also optimal among purified free enzymes (Fig. 3C, Bar 5). Since the kinetics of xylan removal by the employed xylanases is much more higher than the slower cellulose degradation by cellulases used in this study (Fig. S1), it would be therefore logical that a higher cellulase/xylanase ratio would be required for optimized wheat straw deconstruction.

We observed here that the cellulosome paradigm was more efficient than the secreted free-enzyme approach and that elaborate cellulosome structures (consortia 2 and 3) conferred high stability to the catalytic subunits (Table 2) and high cellulose-binding abilities to the bacterial cells (Table 3). The stability of the enzymes seems to be a key parameter in terms of enzymatic efficiency. At later cultivation times (above 48 h) the anchoring paradigm appears more advantageous than the secreted free enzyme paradigm for the same enzymatic composition (Fig. S7). This corresponds to the decrease in stability of the secreted cellulases (Table 2), whereas the anchored enzymes remain fully active. While the cellulosomal machinery is considered to induce synergistic activity among the catalytic modules by their close proximity within the complex (5, 7), the present study as well as others (48, 49) strongly support the importance of the stability conferred upon the enzymes by the scaffoldin subunit.

The ability of the bacteria to utilize the wheat straw substrate as the sole carbon source was assessed on a chemically defined medium. However, wheat straw failed to sustain growth of either the wild-type bacteria or the consortium 2 that produces the highest amount of sugars (data not shown). We further examined the minimal amount of sugar required to sustain growth by growing wild-type *L. plantarum* cells on either glucose, cellobiose, xylose or xylobiose. No growth was observed on pure xylose and xylobiose while the minimal concentration that sustained growth was 0.2% glucose (~11 mM) or 0.2% cellobiose (~5.5 mM) on chemically defined medium (CDM) (Fig. S8). The sugars produced by the best-performing cellulosomal machinery (Fig.3C, bar 2) was about 17 mM of a mixture of soluble sugar products, some of which are not utilizable, and about 4 mM of unconsumed sugars (Fig.3A, bar 2). The lack of growth suggests that the amount and type of sugars produced by the consortia are the limiting factor for growth sustainability. To bridge this gap in future studies, we will screen for additional highly expressed cellulases, in order to generate higher production of sugars that can be assimilated. In addition, it is important to fine-tune the amount and/or types of xylanases, which, on the one hand, serve to remove the embedded xylan that prevents physical access of the cellulases to the cellulose, but, on the other, will produce sugars that are not consumed by the *L. plantarum* cells. The data in Table S2 suggests that xylose may be assimilated by the cells, since low concentrations of xylose were detected in the presence of *L. plantarum*. The complete genome sequence of *L. plantarum* WCFS1 indeed suggests the presence of genes involved in xylose transport but genes for D-xylose isomerase and D-xylose kinase were not detected (50), indicating that xylose cannot be fermented.

Indeed, effective xylose transport was also demonstrated for strain 3NSH, but xylose was not metabolized in these studies (51). Therefore, further research should consider the implementation of xylose assimilation genes in strain WCSF1 as for strain NCIMB 8826 (52). Alternative explanations for the lack of bacterial growth by the cell consortia should be examined in future studies, such as the potential release of cellulase inhibitors by xylanase action (53).

Within the context of gut microbiome ecosystems, the xylan degradation products produced by the cell consortia developed in this work could also benefit the overall microbial community. As a potent gut microbe, the engineering of *L. plantarum* towards fiber degradation could be highly beneficial for clinical applications, such as probiotics (26). Indeed, by enabling this bacterium to degrade plant fiber, we potentially increase its fitness in the gut by extending its status in the ecosystem, which will allow it to better persist as a probiotic organism. Furthermore, the augmented cell-surface display conferred by the adaptor scaffoldin strategy could serve to promote higher efficiency of mucosal vaccines, based on bacteria as delivery vehicles (54).

Material and Methods

All the experiments have been replicated three times in triplicate, and the data served to perform the statistical calculations in the relevant figures and tables.

Cloning. All recombinant proteins employed in this study (see representation in Figure 1) were first cloned into pET28a plasmids and designed to contain a His-tag for subsequent purification by standard restriction-based cloning procedures (55). The

385 recombinant enzymes from *C. papyrosolvens* were produced by replacing their native
386 dockerins with dockerins of different specificities using respective genomic DNA: 5-*g* was
387 obtained by fusing the catalytic module of *C. papyrosolvens* GH5 (GenBank: EPR12097.1)
388 to a dockerin from *Archeoglobus fulgidus* (Orf2375), 9-*b* was obtained by fusing the
389 catalytic module of *C. papyrosolvens* GH9 (GenBank: EPR13542.1) to a dockerin of
390 *Bacteroides cellulosolvens* (ScaA), 10-*t* was obtained by fusing the catalytic module of *C.*
391 *papyrosolvens* GH10 (GenBank: EPR14039.1) to a dockerin of *C. thermocellum* (Cel48S)
392 and 11-*a* was obtained by fusing the catalytic module of *C. papyrosolvens* GH11 (GenBank:
393 EPR13563.1) to a dockerin of *Acetivibrio cellulolyticus* (ScaB).

394 The adaptor scaffoldins Adaptor·1 and Adaptor·2 were obtained by fusing
395 previously employed bivalent scaffoldins (19) to a type II dockerin from *C. thermocellum*
396 (CipA) for Adaptor·1 and to a type III dockerin from *Ruminococcus flavefaciens* 17 (ScaB)
397 for Adaptor·2.

398 The anchoring scaffoldins Anc·2, Anc·3a, Anc·3b and Anc·4 were obtained by fusing
399 one or two type II cohesins from *C. thermocellum* (OlpB) to one or two type III cohesins
400 from *R. flavefaciens* 17 (ScaE), as designated in Figure 1.

401 The enzymes and the genes coding for the two adaptor scaffoldins were introduced
402 into *L. plantarum* using the previously employed pSIP vectors for efficient
403 secretion/attachment of heterologous proteins (21, 22) using the leader peptide (Lp)
404 Lp3050 via pLp_3050sAmy, by replacing the amylase gene in these plasmids by an
405 appropriately amplified gene fragment (31). As the five different anchoring scaffoldins
406 (Anc·1, Anc·2, Anc·3a, Anc·3b and Anc·4) are to be integrated into the bacterial cell wall,

we fused them into the potent cell wall anchor (cwa) anchoring signal cwa2 (22) via the modular pLp_0373sOFA anchoring plasmids (56).

To amplify DNA fragments by PCR for cloning, T-Gradient device (Biometra, Germany) was used. The PCR was performed in 50 µl reaction mixtures.

For short PCR products (up to 500 base pairs), PCR ready mix (Abgen, Epsom, Surrey, UK) was employed. For longer PCR fragments, PCRs were performed using Phusion high-fidelity DNA polymerase F530-S (New England BioLabs, Inc.). Primers were added to a final concentration of 0.5 µM. PCR was programmed according to each manufacturer's instructions. Primers are listed in Table S2 of the supplementary materials.

Protein expression and purification from *Escherichia coli.* Recombinant proteins were expressed in *E. coli* BL21 (DE3) and purified as described earlier (18, 42).

Protein expression in *L. plantarum.* The methodology described in Moraïs et al was followed (22). For the consortia experiments, strains producing either cellulase, xylanase, adaptor or anchoring scaffoldins, were mixed at stoichiometric molar ratios for the enzyme/scaffoldin, and scaffoldin/scaffoldin interactions and then grown on MRS (as prepared by BD Difco™ without protease peptone) supplemented with 40 mM $CaCl_2$.

Western and Far-Western blotting of *L. plantarum* secreted proteins. The methodology described in Moraïs et al was followed (22) for Western Blot experiments (Fig. S4, E and F). In Far-Western Blot (Fig. S4, A, B, C and D), an interaction step was included after blocking. Binding interactions with the blotted proteins were assayed with tagged fusions of specific cohesins fused to the CBM3a module (from the *C. thermocellum* scaffoldin) (CBM-Coh) (57, 58). Specific rabbit antibody against the fused tag (CBM)

diluted at 1:3000 (58, 59) was used as the primary antibody. The Far Western Blot experiments served here to verify both the presence of the full-length dockerin-bearing enzymes and their ability to bind their respective cohesins.

ELISA binding assay. The methodology described in Barak et al was followed (57) with the following modification. MaxiSorp ELISA plates (Nunc A/S, Roskilde, Denmark) were coated overnight at 4°C with 1 µg/ml of either the specific dockerin fused to xylanase T6 from *Geobacillus stearothermophilus* (Xyn-Doc) or the CBM-Coh (100 µl/well) in 0.1 M sodium carbonate (pH 9). After the blocking step, incremental dilutions of either *L. plantarum* washed whole cells, concentrated supernatant fluids (OD_{600}= 1) or 100 ng/ml of purified recombinant proteins in blocking buffer were added. Specific rabbit antibody, raised against either the CBM diluted at 1:3000 in blocking buffer or the type II cohesin from *C. thermocellum* (1:10000 dilution), was used as primary antibody.

Enzymatic activity on pre-treated wheat straw degradation. Prior to enzymatic assay, culture supernatant fluids (for secreted proteins) were concentrated using Amicon centrifugal filters with a 30-kDa cut-off (Millipore, Molsheim, France) and washed with Tris Buffer Saline (TBS x10: 80 g NaCl, 2 g KCl, 30 g Tris, ddw to 1L, adjust pH to 7.4 with HCl 32%) containing 40 mM $CaCl_2$; cells (for anchored designer cellulosomes) were washed with TBS containing 1% Triton X-100 by centrifugation and resuspension to eliminate the sugars present in the MRS medium. Hatched wheat straw, pre-treated with 12% sodium hypochlorite, was prepared as described before (18). This type of pretreatment selectively removes lignin from the biomass, leaving the hemicellulose fraction largely intact. A typical assay mixture consisted of either washed whole cells or

concentrated supernatant fluids from *L. plantarum* at specified concentrations, applied to a suspension of 40 g/liter pre-treated wheat straw in the relevant specified reaction volume (50 mM citrate buffer [pH 6.0], 12 mM $CaCl_2$, 2 mM EDTA). Reactions were incubated at 37°C under shaking. The total amount of sugars released was determined using the dinitrosalicylic acid (DNS) assay as described previously (42, 60).

When pure proteins or designer cellulosomes were employed (Fig. 3C), similar conditions were used with a stoichiometric concentration of enzymes (and scaffoldins), whereby the anchoring scaffoldin was set at 12 nM. The designer cellulosomes were allowed to assemble for 3 h at room temperature with all the enzymatic assay components except the wheat straw substrate. Upon addition of the wheat straw, the enzymatic reaction mixture was incubated for 96 h at 37°C under shaking.

Sugar analysis. Sugar content was analyzed using a high-performance anion-exchange chromatography (HPAEC) system equipped with a PA1 column (Dionex, Sunnyvale, CA). Supernatants of the reaction mixtures obtained after centrifugation were loaded onto the PA1 column, and eluted with 200 mM NaOH (flow rate of 1 ml/min). At first, standards consisting of pure arabinose, xylose, xylobiose, xylotriose, glucose, cellobiose, and cellotriose were loaded separately to determine elution time and peak areas as a function of the sugar concentration. Sugars present in blank were deducted in all the samples.

Stability assay. The stability of the enzymatic combination at 37°C was determined by incubating the described consortia (at 3 nM for each enzyme) without substrate over a 48-h period at 37°C. The residual enzymatic activity was calculated as the

relative activity of the consortium incubated at 37°C compared to that of the anchored consortium (washed whole cells) or secreted consortium (concentrated supernatant fluids) that was directly introduced to the substrate (with no incubation period), on carboxymethyl cellulose (CMC) or beechwood xylan for a period of 2 hours at 37°C.

Adherence/turbidity assay. Wild-type *L. plantarum* bacteria or consortia of transformed strains were grown with inducer until OD_{600}=1. A volume of 1 mL of the cultures was then subjected to interaction with 30 mg of Avicel for 1h at 4°C in TBS supplemented with 40 mM $CaCl_2$. Gentle centrifugation (about 1 min at 1000 rpm) was then performed to separate the Avicel substrate. The absorbance at OD_{600} was then verified, using MRS medium supplemented with Avicel under the same conditions as a blank without bacterial cells. The difference in absorbance at OD_{600} reflects the adhesion of the cells to cellulose.

Bacterial growth. A chemically defined medium (CDM) as developed by Wegkamp et al (61) was prepared with 20 g/l pre-treated wheat straw. In parallel, consortium 2 or the wild-type bacteria were cultured in MRS without protease peptone as described above. Cells were harvested, washed twice in 10 ml 0.85% NaCl and 10 mM $CaCl_2$, and the washed cells served as an inoculum of the CDM containing wheat straw as carbon source. The medium was supplemented with pSIP inducer, 10 mM $CaCl_2$, and erythromycin in the case of consortium 2. Growth at 37°C under agitation (200 rpm) was followed for a week by measuring the OD at 600 nm of the supernatant culture after the wheat straw precipitated (5 min). Growth of the wild-type bacteria was assessed on CDM supplemented with 0 to 1% of either cellobiose, glucose, xylose or xylobiose.

Funding information

The research was supported by grants from the Israel Science Foundation (No. 1313/13 to IM and 1349/13 to EAB), by the Israeli Chief Scientist Ministry of Agriculture and Rural Development Fund (No. 362-0426) to EAB and IM, by the Israeli Chief Scientist Ministry of Science Foundation (No.3-10880) to EAB and IM, by the European Research Council (No. 640384) to IM, and by the United States-Israel Binational Science Foundation (BSF). The authors appreciate the support of the European Union, CellulosomePlus (No. 604530) and European Union Horizon 2020: Waste2Fuels. EAB is the incumbent of The Maynard I. and Elaine Wishner Chair of Bio-organic Chemistry.

REFERENCES

1. Doblin MS, Pettolino F, Bacic A. 2010. Evans Review : Plant cell walls: the skeleton of the plant world. Funct Plant Biol 37:357.
2. Artzi L, Bayer EA, Moraïs S. 2016. Cellulosomes: bacterial nanomachines for dismantling plant polysaccharides. Nat Rev Microbiol.
3. Lamed R, Setter E, Bayer EA. 1983. Characterization of a cellulose-binding, cellulase-containing complex in *Clostridium thermocellum*. J Bacteriol 156:828–36.
4. Shoham Y, Lamed R, Bayer EA. 1999. The cellulosome concept as an efficient microbial strategy for the degradation of insoluble polysaccharides. Trends Microbiol 7:275–281.
5. Bayer EA, Belaich J-P, Shoham Y, Lamed R. 2004. The Cellulosomes: Multienzyme Machines For Degradation Of Plant Cell Wall Polysaccharides. Annu Rev Microbiol 58:521–554.
6. Adams JJ, Pal G, Jia Z, Smith SP. 2006. Mechanism of bacterial cell-surface attachment revealed by the structure of cellulosomal type II cohesin-dockerin complex. Proc Natl Acad Sci U S A 103:305–310.
7. Bayer EA, Setter E, Lamed R. 1985. Organization and distribution of the cellulosome in *Clostridium thermocellum*. J Bacteriol 163:552–9.
8. Tsai S-L, Oh J, Singh S, Chen R, Chen W. 2009. Functional assembly of minicellulosomes on the *Saccharomyces cerevisiae* cell surface for cellulose hydrolysis and ethanol production. Appl Environ Microbiol 75:6087–93.
9. Tsai S-L, Goyal G, Chen W. 2010. Surface display of a functional minicellulosome by intracellular complementation using a synthetic yeast consortium and its application to cellulose hydrolysis and ethanol production. Appl Environ Microbiol 76:7514–20.
10. Wen F, Sun J, Zhao H. 2010. Yeast surface display of trifunctional minicellulosomes for simultaneous Saccharification and fermentation of cellulose to ethanol. Appl Environ

Microbiol 76:1251–1260.

11. Lilly M, Fierobe H-P, van Zyl WH, Volschenk H. 2009. Heterologous expression of a *Clostridium* minicellulosome in *Saccharomyces cerevisiae*. FEMS Yeast Res 9:1236–49.

12. You C, Zhang X-Z, Sathitsuksanoh N, Lynd LR, Zhang Y-HP. 2012. Enhanced microbial utilization of recalcitrant cellulose by an ex vivo cellulosome-microbe complex. Appl Environ Microbiol 78:1437–44.

13. Anderson TD, Robson S a., Jiang XW, Malmirchegini GR, Fierobe HP, Lazazzera BA, Clubb RT. 2011. Assembly of minicellulosomes on the surface of *Bacillus subtilis*. Appl Environ Microbiol 77:4849–4858.

14. Willson BJ, Kovács K, Wilding-Steele T, Markus R, Winzer K, Minton NP. 2016. Production of a functional cell wall-anchored minicellulosome by recombinant *Clostridium acetobutylicum* ATCC 824. Biotechnol Biofuels 9:109.

15. Wieczorek AS, Martin VJJ. 2010. Engineering the cell surface display of cohesins for assembly of cellulosome-inspired enzyme complexes on *Lactococcus lactis* . Microb Cell Fact 9:69.

16. Bayer EA, Morag E, Lamed R. 1994. The cellulosome — A treasure-trove for biotechnology. Trends Biotechnol 12:378–386.

17. Fierobe H, Mingardon F, Mechaly A, Be A, Rincon MT, Lamed R, Tardif C, Be J, Bayer EA. 2005. Action of Designer Cellulosomes on Homogeneous Versus Complex substrates 280:16325–16334.

18. Moraïs S, Morag E, Barak Y, Goldman D, Hadar Y, Lamed R, Shoham Y, Wilson DB, Bayer EA. 2012. Deconstruction of lignocellulose into soluble sugars by native and designer cellulosomes. MBio 3:1–11.

19. Moraïs S, Barak Y, Caspi J, Hadar Y, Lamed R, Shoham Y, Wilson DB, Bayer EA. 2010.

554 Cellulase-xylanase synergy in designer cellulosomes for enhanced degradation of a
555 complex cellulosic substrate. MBio 1:e00285-10.
556 20. Huang GL, Anderson TD, Clubb RT. 2013. Engineering microbial surfaces to degrade
557 lignocellulosic biomass. Bioengineered 5:1–11.
558 21. Moraïs S, Shterzer N, Grinberg IR, Mathiesen G, Eijsink VGH, Axelsson L, Lamed R, Bayer E
559 a., Mizrahi I. 2013. Establishment of a simple *Lactobacillus plantarum* cell consortium for
560 cellulase-xylanase synergistic interactions. Appl Environ Microbiol 79:5242–5249.
561 22. Moraïs S, Shterzer N, Lamed R, Bayer EA, Mizrahi I. 2014. A combined cell-consortium
562 approach for lignocellulose degradation by specialized *Lactobacillus plantarum* cells.
563 Biotechnol Biofuels 7:112.
564 23. Mazzoli R, Bosco F, Mizrahi I, Bayer EA, Pessione E. 2014. Towards lactic acid bacteria-
565 based biorefineries. Biotechnol Adv 32:1216–1236.
566 24. G-Alegría E, López I, Ruiz JI, Sáenz J, Fernández E, Zarazaga M, Dizy M, Torres C, Ruiz-Larrea
567 F. 2004. High tolerance of wild *Lactobacillus plantarum* and *Oenococcus oeni* strains to
568 lyophilisation and stress environmental conditions of acid pH and ethanol. FEMS Microbiol
569 Lett 230:53–61.
570 25. Lucena BT, dos Santos BM, Moreira JL, Moreira APB, Nunes AC, Azevedo V, Miyoshi A,
571 Thompson FL, de Morais M. 2010. Diversity of lactic acid bacteria of the bioethanol
572 process. BMC Microbiol 10:298.
573 26. Walter J. 2008. Ecological role of *Lactobacilli* in the gastrointestinal tract : implications for
574 fundamental and biomedical research. Appl Env Microbiol 74:4985–4996.
575 27. Martino ME, Bayjanov JR, Caffrey BE, Wels M, Joncour P, Hughes S, Gillet B, Kleerebezem
576 M, Lyon CB. 2016. Nomadic lifestyle of *Lactobacillus plantarum* revealed by comparative
577 genomics of 54 strains isolated from different habitats. Env Microbiol 18:4974–4989.

28. Storelli G, Defaye A, Erkosar B, Hols P, Royet J, Leulier F. 2017. *Lactobacillus plantarum* Promotes *Drosophila* Systemic Growth by Modulating Hormonal Signals through TOR-Dependent Nutrient Sensing. Cell Metab 14:403–414.

29. Sharon G, Segal D, Ringo JM, Hefetz A, Zilber-Rosenberg I, Rosenberg E. 2010. Commensal bacteria play a role in mating preference of *Drosophila melanogaste*r. Proc Natl Acad Sci 107:20051–20056.

30. Schwarzer M, Makki K, Storelli G, Machuca-Gayet I, Srutkova D, Hermanova P, Martino ME, Balmand S, Hudcovic T, Heddi A, Rieusset J, Kozakova H, Vidal H, Leulier F. 2016. *Lactobacillus plantarum* strain maintains growth of infant mice during chronic undernutrition. Science (80-) 351:854 LP-857.

31. Mathiesen G, Sveen A, Brurberg MB, Fredriksen L, Axelsson L, Eijsink VG. 2009. Genome-wide analysis of signal peptide functionality in *Lactobacillus plantarum* WCFS1. BMC Genomics 10:425.

32. Xu Q, Gao W, Ding S, Kenig R, Shoham Y, Bayer EA, Lamed R. 2003. The cellulosome system of *Acetivibrio cellulolyticus* includes a novel type of adaptor protein and a cell surface anchoring protein. J Bacteriol 185:4548–57.

33. Artzi L, Dassa B, Borovok I, Shamshoum M, Lamed R, Bayer EA. 2014. Cellulosomics of the cellulolytic thermophile *Clostridium clariflavum*. Biotechnol Biofuels 7:100.

34. Zepeda V, Dassa B, Borovok I, Lamed R, Bayer EA, Cate JHD. 2013. Draft Genome Sequence of the Cellulolytic Bacterium *Clostridium papyrosolvens C7* (ATCC 700395). Genome Announc.

35. Mingardon F, Chantal A, López-Contreras AM, Dray C, Bayer EA, Fierobe H-P. 2007. Incorporation of fungal cellulases in bacterial minicellulosomes yields viable, synergistically acting cellulolytic complexes. Appl Environ Microbiol 73:3822–3832.

602 36. Fan L-H, Zhang Z-J, Yu X-Y, Xue Y-X, Tan T-W. 2012. Self-surface assembly of cellulosomes
603 with two miniscaffoldins on *Saccharomyces cerevisiae* for cellulosic ethanol production.
604 Proc Natl Acad Sci 109:13260–13265.
605 37. Blouzard JC, Bourgeois C, De Philip P, Valette O, Bélaïch A, Tardif C, Bélaïch JP, Pagès S.
606 2007. Enzyme diversity of the cellulolytic system produced by *Clostridium cellulolyticum*
607 explored by two-dimensional analysis: Identification of seven genes encoding new
608 dockerin-containing proteins. J Bacteriol 189:2300–2309.
609 38. Mohand-Oussaid O, Payot S, Guedon E, Gelhaye E, Youyou A, Petitdemange H. 1999. The
610 extracellular xylan degradative system in *Clostridium cellulolyticum* cultivated on xylan :
611 evidence for cell-free cellulosome production. J Bacteriol 181:4035–4040.
612 39. Haimovitz R, Barak Y, Morag E, Voronov-Goldman M, Lamed R, Bayer EA. 2008. Cohesin-
613 dockerin microarray: Diverse specificities between two complementary families of
614 interacting protein modules. Proteomics 8:968–979.
615 40. Pagès S, Belaich A, Belaich J-P, Morag E, Lamed R, Shoham Y, Bayer EA. 1997. Species-
616 specificity of the cohesin-dockerin interaction between *Clostridium thermocellum* and
617 *Clostridium cellulolyticum*: Prediction of specificity determinants of the dockerin domain.
618 Proteins 29:517–527.
619 41. Tsai SL, DaSilva NA, Chen W. 2013. Functional display of complex cellulosomes on the yeast
620 surface via adaptive assembly. ACS Synth Biol 2:14–21.
621 42. Stern J, Moraïs S, Lamed R, Bayer EA. 2016. Adaptor scaffoldins: An original strategy for
622 extended designer cellulosomes, inspired from nature. MBio 7(2):e00083-16.
623 43. Remus DM, Bongers RS, Meijerink M, Fusetti F, Poolman B, de Vos P, Wells JM,
624 Kleerebezem M, Bron PA. 2013. Impact of *Lactobacillus plantarum* sortase on target
625 protein sorting, gastrointestinal persistence, and host immune response modulation. J

626 Bacteriol 195:502–509.
627 44. Bayer E a, Lamed R, Himmel ME. 2007. The potential of cellulases and cellulosomes for
628 cellulosic waste management. Curr Opin Biotechnol 18:237–45.
629 45. Bosma EF, Forster J, Nielsen AT. 2017. *Lactobacilli* and *Pediococci* as versatile cell factories
630 – Evaluation of strain properties and genetic tools. Biotechnol Adv 35:419–442.
631 46. Lynd L, Zyl W, Mcbride J, Laser M. 2005. Consolidated bioprocessing of cellulosic biomass:
632 an update. Curr Opin Biotechnol 16:577–583.
633 47. Agapakis CM, Boyle PM, Silver P a. 2012. Natural strategies for the spatial optimization of
634 metabolism in synthetic biology. Nat Chem Biol 8:527–535.
635 48. Krauss J, Zverlov V V., Schwarz WH. 2012. In vitro reconstitution of the complete
636 *Clostridium thermocellum* cellulosome and synergistic activity on crystalline cellulose. Appl
637 Environ Microbiol 78:4301–4307.
638 49. Xu C, Qin Y, Li Y, Ji Y, Huang J, Song H, Xu J. 2010. Factors influencing cellulosome activity
639 in consolidated bioprocessing of cellulosic ethanol. Bioresour Technol 101:9560–9.
640 50. Kleerebezem M, Boekhorst J, van Kranenburg R, Molenaar D, Kuipers OP, Leer R, Tarchini
641 R, Peters SA, Sandbrink HM, Fiers MW, Stiekema W, Lankhorst RM, Bron PA, Hoffer SM,
642 Groot MN, Kerkhoven R, de Vries M, Ursing B, de Vos WM, Siezen RJ. 2003. Complete
643 genome sequence of *Lactobacillus plantarum* WCFS1. Proc Natl Acad Sci U S A2003/02/05.
644 100:1990–1995.
645 51. Heiss S, Hörmann A, Tauer C, Sonnleitner M, Egger E, Grabherr R, Heinl S. 2016. Evaluation
646 of novel inducible promoter/repressor systems for recombinant protein expression in
647 *Lactobacillus plantarum*. Microb Cell Fact 15:50.
648 52. Okano K, Yoshida S, Yamada R, Tanaka T, Ogino C, Fukuda H, Kondo A. 2009. Improved
649 production of homo-D-lactic acid via xylose fermentation by introduction of xylose

650 assimilation genes and redirection of the phosphoketolase pathway to the pentose
651 phosphate pathway in L-Lactate dehydrogenase gene-deficient *Lactobacillus plantarum*.
652 Appl Env Microbiol2009/10/13. 75:7858–7861.
653 53. Zhang J, Tang M, Viikari L. 2012. Xylans inhibit enzymatic hydrolysis of lignocellulosic
654 materials by cellulases. Bioresour Technol 121:8–12.
655 54. Fredriksen L, Kleiveland CR, Hult LTO, Lea T, Nygaard CS, Eijsink VGH, Mathiesen G. 2012.
656 Surface Display of N-Terminally Anchored Invasin by *Lactobacillus plantarum* Activates NF-
657 kB in Monocytes. Appl Env Microbiol 78:5864–5871.
658 55. Peleg Y, Unger T. 2014. DNA Cloning and Assembly Methods, p. 73–87. *In* Valla, S, Lale, R
659 (eds.), Methods in Molecular Biology. Springer Science+Business Media, New York.
660 56. Fredriksen L, Mathiesen G, Sioud M, Eijsink VGH. 2010. Cell wall anchoring of the 37-
661 kilodalton oncofetal antigen by *Lactobacillus plantarum* for mucosal cancer vaccine
662 delivery. Appl Environ Microbiol 76:7359–62.
663 57. Barak Y, Handelsman T, Nakar D, Mechaly A, Lamed R, Shoham Y, Bayer EA. 2005. Matching
664 fusion-protein systems for affinity analysis of two interacting families of proteins: The
665 cohesin-dockerin interaction. J Mol Recognit 18:491–501.
666 58. Lapidot A, Mechaly A, Shoham Y. 1996. Overexpression and single-step purification of a
667 thermostable xylanase from *Bacillus stearothermophilus* T-6. J Biotechnol 51:259–264.
668 59. Morag E, Lapidot A, Govorko D, Lamed R, Wilchek M, Bayer EA, Shoham Y. 1995.
669 Expression, purification and characterization of the cellulose-binding domain of the
670 scaffoldin subunit from the cellulosome of *Clostridium thermocellum*. Appl Environ
671 Microbiol 61:1980–1986.
672 60. Miller GL. 1959. Use of dinitrosalicylic acid reagent for determination of reducing sugar.
673 Anal Biochem 31:426–428.

674 61. Wegkamp A, Teusink B, Vos WM De, Smid EJ. 2010. Development of a minimal growth
675 medium for *Lactobacillus plantarum*. Lett Appl Microbiol 50:57–64.
676
677

FIGURES

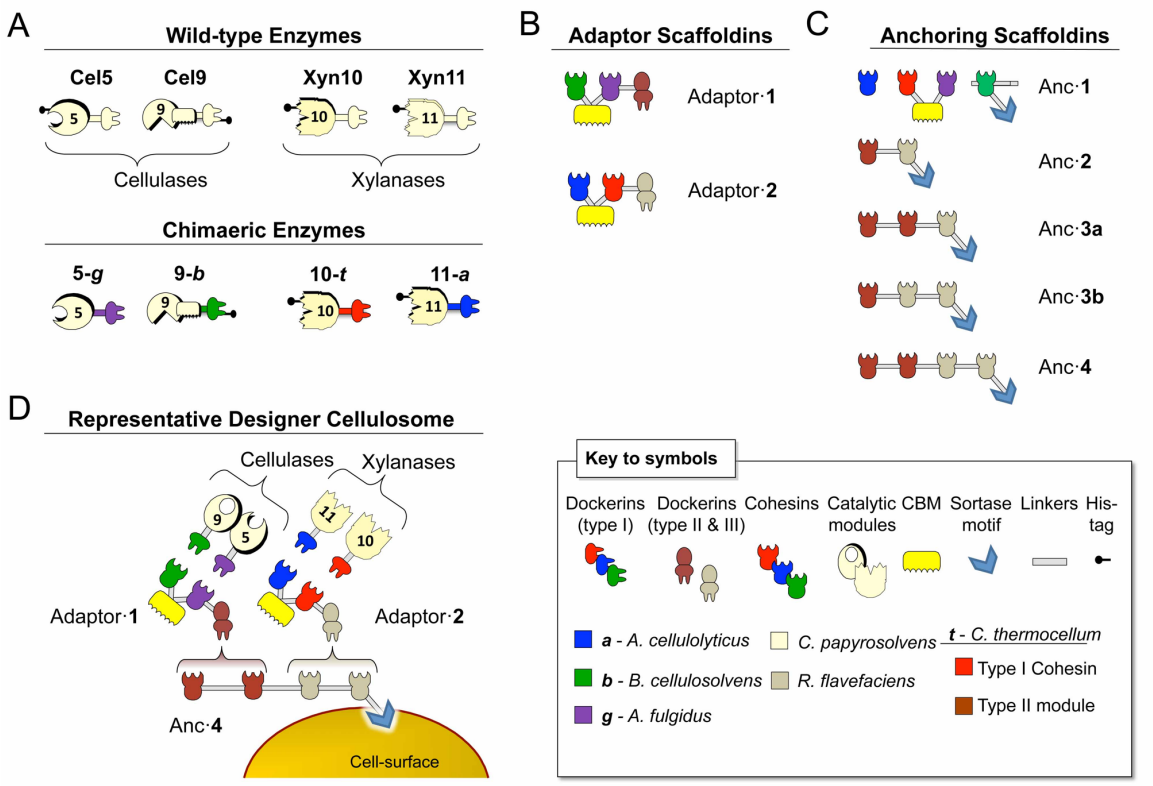

Fig. 1. Schematic representation of the wild-type and chimaeric proteins used in this study. The bacterial species from which the representative modules are derived are shown color-coded in the pictograms. (A) Wild-type and chimaeric *C. papyrosolvens* enzymes. In the shorthand notation for the recombinant enzymes, the numbers 5, 9, 10 and 11 correspond to the GH family of the respective catalytic modules; the origin of a given dockerin module is also indicated by lowercase italic characters, found in the Key to symbols. (B) Modular architectures of the two different adaptor scaffoldins designed for this work. Each adaptor scaffolding contains two divergent cohesins for selective integration of different dockerin-containing enzymes and a type II or type III dockerin for attachment to the appropriate cohesin-containing anchoring scaffoldin. (C) Modular architectures of the various types of anchoring scaffoldins designed in this study. Each contains a C-terminal sortase signal motif for covalent attachment to the cell surface. Anc·1 contains 4 divergent cohesins for selective integration of 4 different dockerin-bearing enzymes. Anc·2 through Anc·4 are anchoring scaffoldins differing in numbers (2–4) or positions (3a, 3b) of cohesins that integrate the two adaptor scaffoldins and their resident enzymes. (D) Example of designer cellulosome assembly, resulting from a consortium of different strains of transformed *L. plantarum*.

A

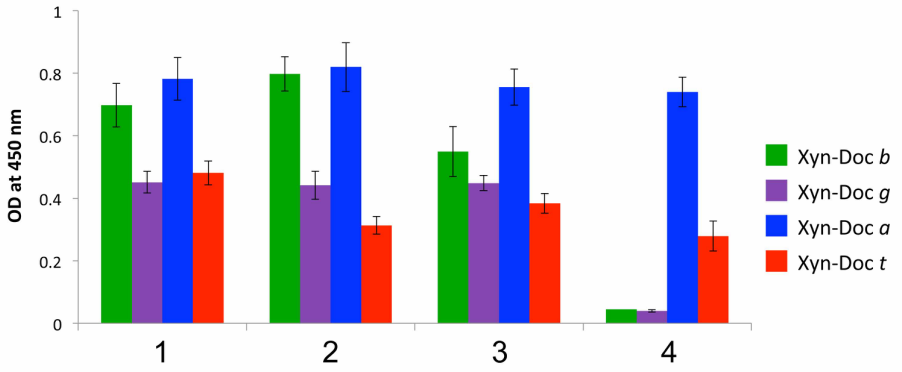

B

Consortium	Anchoring scaffoldin	Adaptor scaffoldin	Potential for enzyme integration	Scheme
1	Anc·**2**	Adaptor·**1** Adaptor·**2**	2 Cellulases + 2 Xylanases	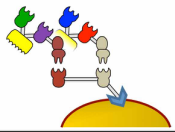
2	Anc·**3a**	Adaptor·**1** *(2 units)* Adaptor·**2**	4 Cellulases + 2 Xylanases	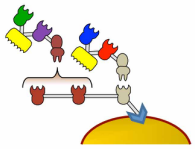
3	Anc·**3b**	Adaptor·**1** Adaptor·**2** *(2 units)*	2 Cellulases + 4 Xylanases	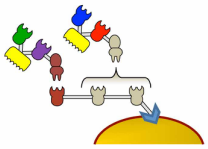
4	Anc·**1**	None	2 Cellulases + 2 Xylanases	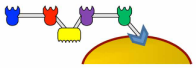

Fig. 2. ELISA-based binding assay demonstrating the presence of active cohesin modules on the *L. plantarum* cell surface. (A) The three different consortia of individually transformed *L. plantarum* cells (see panel B for description) and the individual *L. plantarum* strain transformed with the gene for anchoring scaffoldin Anc·1 were examined for their capacity to interact with specific dockerin-bearing fusion proteins. Microtiter plates were coated with 1 μg/ml of the specified dockerins fused to the carrier protein (xylanase T6 from *G. stearothermophilus*). Washed whole bacterial cells from transformed lactobacilli of the different consortia and the Anc·1-bearing strain were then allowed to interact. The primary antibody used was prepared against the CBM module of the scaffoldins. Washed bacterial cells (wild-type *L. plantarum*) served as a control. (B) Description of the incorporated chimaeric scaffoldins for the indicated cellulosome complex. The different cell consortia comprised the following: (1) consortium of anchoring scaffoldin Anc·2 with Adaptor·1 and Adaptor·2 (one copy each); (2) consortium of anchoring scaffoldin Anc·3a with 2 copies of Adaptor·1 and one copy of Adaptor·2; (3) consortium of anchoring scaffoldin Anc·3b with 1 copy of Adaptor·1 and two copies of Adaptor·2; (4) anchoring scaffoldin Anc·1.

A. *L. plantarum* cell consortia *(in vivo)*

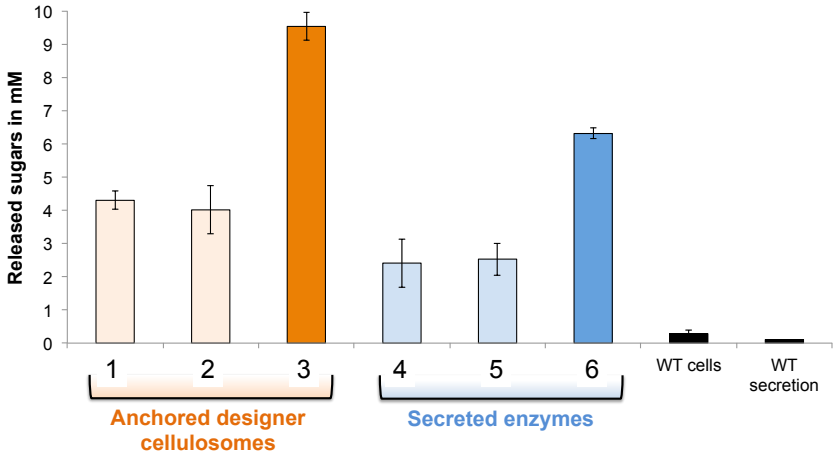

B. Composition of consortia and enzymes

Consortium	1	2	3	4	5	6
Chimaeric enzymes – 1 unit of each enzyme = 3 nM						
Xylanases 11-*a*, 10-*t*	1 unit	1 unit	2 units	1 unit	1 unit	2 units
Cellulases 9-*b*, 5-*g*	1 unit	2 units	1 unit	1 unit	2 units	1 unit
Total enzymatic concentration	**12 nM**	**18 nM**	**18 nM**	**12 nM**	**18 nM**	**18 nM**
Chimaeric scaffoldins – 1 unit of each scaffoldin = 3 nM						
Anc·2	1 unit					
Anc·3a		1 unit				
Anc·3b			1 unit			
Adaptor·1	1 unit	2 units	1 unit			
Adaptor·2	1 unit	1 unit	2 units			

***In vitro* designer cellulosomes** **Free enzymes**

C. Purified designer cellulosomes and free enzymes (in vitro)

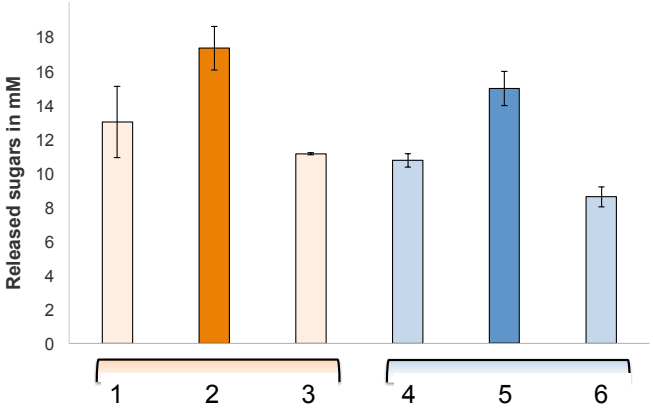

711

Fig. 3. Comparative analysis of the hydrolysis of hypochlorite-pretreated wheat straw by free enzymes versus cell-associated and cell-free designer cellullosomes. (A) Soluble sugars produced in the extracellular medium by different transformed *L. plantarum* consortia versus the wild-type (WT) strain. Reactions were incubated for 96 h at 37°C. For consortia 1, 2, 3 and WT cells, washed cells were used in the enzymatic reaction, whereas for Consortia 4, 5, 6 and WT secretion cells, concentrated supernatant fluids were used. Hypochlorite-pretreated wheat straw was used at a concentration of 40 g/l, and enzymatic activities are represented by the concentration of total reducing sugars (mM). Experiments were conducted three times with triplicate samples, and standard deviations are indicated. (B) The recombinant enzymes and chimaeric scaffoldins that were introduced in the different *L. plantarum* consortia are indicated, and correspond for the respective bars in the chart. The molar ratios between the proteins, the number of units and total enzyme concentration are stipulated. (C) Soluble sugars produced by recombinant cell-free designer cellulosome assemblies and free enzyme mixtures parallel to the ones used in (A), assembled from purified proteins produced by *E. coli.* The cellulosomal components were assembled stoichiometrically, where the concentration of the anchoring scaffoldin was set at 12 nM. The designer cellulosomes were allowed to assemble for 3 h at room temperature with all components of the enzymatic assay except the wheat straw substrate. The enzymatic reaction was incubated for 96 h at 37°C under shaking. Experiments were conducted three times with triplicate samples, and standard deviations are indicated.

Supplementary Table Legends

Table S1. Carbohydrate analysis of remaining sugars after enzymatic degradation of pre-treated hatched wheat straw by various *L. plantarum* consortia over a 96-h incubation.

Enzyme combination	**µM of released sugar ± SD**						
	Arabinose	Glucose	Xylose	Xylobiose	Cellobiose	Xylotriose	Cellotriose
Anchoring 1	198 ±10	441 ±21	159 ±11	1794 ±122	4 ±0	503 ±17	150 ±14
Anchoring 2	102 ±7	336 ±27	58 ±4	592 ±42	42 ±1	243 ±5	81 ±18
Anchoring 3	27 ±1	672 ±39	94 ±8	5034 ±145	4 ±0	1870 ±126	32 ±2
Secreting 4	60 ±9	75 ±1	29 ±2	1861 ±17	7 ±0	1134 ±102	257 ±13
Secreting 5	101 ±17	109 ±5	142 ±30	1926 ±184	ND	1164 ±131	182 ±28
Secreting 6	100 ±8	162 ±9	25 ±6	2520 ±222	ND	1773 ±154	207 ±11

ND, not detected

739 **Table S2:** Primer tables

740

Chimearas (plasmid)	Modules	Primers	Sequence	Restriction enzyme
***C. papyrosolvens* chimaeric enzymes**				
9-*b* (pET-28a)	Catalytic subunit GH9	Forward	5'GCATTA**TCATGA**GCGCAGGAA CATATAATTATGGAG 3'	BspHI
		Reverse	5'CCATTA**GCTAGC**ATCAGGGTT TTCCGGTCCACC 3'	NheI
	Dockerin *b*	Forward	5'ATACAA**GCTAGC**CCAAAAGGC ACAGCTACAGTAT 3'	NheI
		Reverse	5'AGGCTA**CTCGAG**CGCTTTTTG TTCTGCTGGGAAC 3'	XhoI
9-*b* pLp_2588s	Signal peptide 2588	Forward	5'CAAGGT**CATATG**CGCAAAAAA TGGCGATGGTTATT 3'	NdeI
		Reverse	5'AATCCA**GTCGAC**GTTGCGGGC CTGACTAACTAAG 3'	SalI
	Enzymatic subunit 9-*b*	Forward	5'AATGCA**GTCGAC**GCAGGAACA TATAATTATGGAG 3'	SalI
		Reverse	5'GACCTA**AAGCTT**TTACGCTTTT TG TTCTGCTGGGAAC 3'	HindIII
5-*g* (pET-28a)	Catalytic subunit GH5	Forward	5'CCTAAT**CCATGG**GTTATGATG CTTCACTTATTCCG 3'	NcoI
		Reverse	5'AGGCAT**GGTACC**TTATCAGTC TGCGCTTCGAAAGC 3'	KpnI
	Dockerin *g*	Forward	5'TGGACA**GGTACC**AGAAGAAG CA AACAAGGGAGATG 3'	KpnI
		Reverse	5'AATATA**CTCGAG**CTTACCCAG TAAGCCATTCTGG 3'	XhoI
5-*g* pLp_2588s	Signal peptide 2588	*see above (5-g)*		
	Enzymatic unit 5-*g*	Forward	5'AATGCA**GTCGAC**TATGATGCT TCACTTATTCCG 3'	SalI
		Reverse	5'GAACTA**AAGCTT**TTACTTACC CAGTAAGCCATTCTG 3'	HindIII
11-*a* (pET-21a)	Catalytic subunit GH11	Forward	5'CTGGAT**GCTAGC**ATGCACCAT CACCATCACCACGCAACAACGA TTACTGAAAATC 3'	NheI
		Reverse	5'ATCATC**GAGCTC**AGGCTGAGT TCCGCCGCCAAC 3'	SacI
	Dockerin *a*	Forward	5'ATTAGC**GAGCTC**ACAGCAACT ACAACACCAACTACA 3'	SacI
		Reverse	5'CAACGT**CTCGAG**TTATTCTTCT TTCTCTTCAAC 3'	XhoI

11-*a* pLp_3050s	Signal peptide 3050	*from previous publication* [1]		
	Enzymatic unit 11-*a*	Forward	5'CAGAAC**GTCGAC**GCAACAACG ATTACTGAAAATC 3'	SalI
		Reverse	5'AACTTA**AAGCTT**TTATTCTTCT TTCTCTTCAACAGG 3'	HindIII
10-*t* (pET-28a)	Catalytic subunit GH10	Forward	5'GAATTC**CCATGG**GCGCTACTC CAACAGGTACAAGG 3'	NcoI
		Reverse	5'AGACTA**AAGCTT**TGTAGGAGC TGTAGCGAGAGC 3'	HindIII
	Dockerin *t*	Forward	5'AATAGC**AAGCTT**GAAAGCAGT TCCACAGGTCTG 3'	HindIII
		Reverse	5'CCATCA**CTCGAG**TCCGGGGAA CTCTGTAATAATG 3'	XhoI
10-*t* pLp_3050s	Signal peptide 3050	*from previous publication* [1]		
	Enzymatic unit 10-*t*	Forward	5'ATTCCA**GTCGAC**GCTACTCCA ACAGGTACAAGG 3'	SalI
		Reverse	5'AAGCGA**CCCGGG**TTATCCGGG GAACTCTGTAATAATG 3'	SmaI
Chimaeric scaffoldins				
Adaptor·1 (pET-28a)	Cohesin B, CBM3a, cohesin G*	Forward	5'GCAATC**CCATGG**GCGGGAAAA GTTCACCAGGAAATAA3'	NcoI
		Reverse	5'GATCAA**AGATCT**GGCTTCTTC CTGAGAGACAATC3'	BglII
	Dockerin type II *(C. thermocellum)*	Forward	5'TGCACC**GGATCC**AACTAATAA ACC TGTAATAGAAG 3'	BamHI
		Reverse	5'AAAGTC**CTCGAG**CTGTGCGTC GTAATCACTTG 3'	XhoI
Adaptor·1 (pLp_3050s)	Cohesin B, CBM3a, cohesin G, dockerin type II *(C. thermocellum)*	Forward	5'GCATAA**GTCGAC**GGGAAAAGT TCACCAGGAAATAA3'	SalI
		Reverse	5'AAGATC**CCCGGG**TCACTGTGC GTCGTAATCACTTGATG3'	SmaI
Adaptor·2 (pET-28a)	Cohesin A, CBM3a, cohesin T*	Forward	5'CTAACG**CCATGG**GCTTACAGG TTGACATTGGAAGTAC3'	NcoI
		Reverse	5'GATCAG**GCTAGC**AACATTTAC TCCACCGTCAAAG3'	NheI
	Dockerin type III *(R. flavefaciens 17)*	Forward	5'CAATGC**GCTAGC**GCTAACTAC GATCACTCCTACG3'	NheI
		Reverse	5'ACCTGG**CTCGAG**TTTACCGAA TCTTGCGTCTCCG3'	XhoI
Adaptor·2 (pLp_3050s)	Cohesin A, CBM3a, cohesin F, dockerin type III *(R. flavefaciens 17)*	Forward	5'ACTGTA**GTCGAC**TTACAGGTT GACATTGGAAGTAC3'	SalI
		Reverse	5'TCAGAA**CCCGGG**TCATTTACC GAATCTTGCGTCTCCG3'	SmaI
ScAnc·1 (pET-28a)	Cohesin A, CBM3a, cohesins T, G, B**	Forward	5'CAATTG**CCATGG**GCCGGCCGC ATTTACAGGTTGAC3'	NcoI

		Reverse	5’ATTGGC**CTCGAG**TCAAATTGG CTTATTAGTTACAGTAATG3’	XhoI
ScAnc·1 (pLp_0373sOF A)	Cohesin A, CBM3a, Cohesins T, G, B**	Forward	5’AACGCT**GTCGAC**CGGCCGCAT TTACAGGTTGAC3’	SalI
		Reverse	5’GATTCA**ACGCGT**AATTGGCTT ATTAGTTACAGTAATG3’	MluI
ScAnc·2 (pET-28a)	Cohesin T_2 (*OlpB*)	Forward	5’GTTAAA**CCATGG**GCGAAGCAA CTCCAAGTATTGAAATG 3’	NcoI
		Reverse	5’CAAATC**GAATTC**GCTGGCGTC TTTTAACGGTTCTG 3’	EcoRI
	Cohesin F_3 (*ScaE*)	Forward	5’GTTACA**GAATTC**GGCCCCGCT GCTGGTCAGGC 3’	EcoRI
		Reverse	5’CTTAGT**CTCGAG**AGATGTAGT ACTCTCAACCTGG 3’	XhoI
ScAnc·2 (pLp_0373sOF A)	Cohesins T_2, F_3	Forward	5’CATGAA**GTCGAC**GAAGCAACT CCAAGTATTGAAATG 3’	SalI
		Reverse	5’ATAGCA**ACGCGT**AGATGTAGT ACTCTCAACCTGG 3’	MluI
ScAnc·3a (pET-28a)	Cohesins $2T_2$ (*OlpB*)	Forward	5’GTTAAA**CCATGG**GCGAAGCAA CTCCAAGTATTGAAATG 3’	NcoI
		Reverse	5’CAAATC**GAATTC**CGGTACAGG CTCTTCTGTCGG 3’	EcoRI
	Cohesin F_3 (*ScaE*)	*see above (*ScAnc·T_2F_3*)*		
ScAnc·3a (pLp_0373sOF A)	Cohesins $2T_2$, F_3	Forward	5’CATGAA**GTCGAC**GAAGCAACT CCAAGTATTGAAATG 3’	SalI
		Reverse	5’ATAGCA**ACGCGT**AGATGTAGT ACTCTCAACCTGG 3’	MluI
ScAnc·3b (pET-28a)	Cohesins T_2, F_3	Forward	5’GTTAAA**CCATGG**GCGAAGCAA CTCCAAGTATTGAAATG 3’	NcoI
		Reverse	5’CAAATC**GCTAGC**AGATGTAGT ACTCTCAACCTGG 3’	NheI
	Linker Ct-CipA, Cohesin F_3 (*ScaE*)	Forward	5’AACGCT**GCTAGC**GGTAGTTCC GTACCGACAACACAGCCAAATG TTCCGTCAGACGGCCCCGCTGCT GGTCAGGC 3’	NheI
		Reverse	5’CTTAGT**CTCGAG**AGATGTAGT ACTCTCAACCTGG 3’	XhoI
ScAnc·3b (pLp_0373sOF A)	Cohesins T_2, $2F_3$	Forward	5’CATGAA**GTCGAC**GAAGCAACT CCAAGTATTGAAATG 3’	SalI
		Reverse	5’ATAGCA**ACGCGT**AGATGTAGT ACTCTCAACCTGG 3’	MluI
ScAnc·4 (pET-28a)	Cohesins $2T_2$, F_3	Forward	5’GTTAAA**CCATGG**GCGAAGCAA CTCCAAGTATTGAAATG 3’	NcoI
		Reverse	5’CAAATC**GCTAGC**AGATGTAGT ACTCTCAACCTGG 3’	NheI
	Linker Ct-CipA, Cohesin F_3 (*ScaE*)	*see above (*ScAnc·$T_2$2F_3*)*		
ScAnc·4	Cohesins $2T_2$, $2F_3$	Forward	5’CATGAA**GTCGAC**GAAGCAACT CCAAGTATTGAAATG 3’	SalI

(pLp_0373sOFA)		Reverse	5'ACCTAC**ACGCGT**GTGCTCGAG AGATGTAGTAC 3'	MluI

741

742

743

744 The different modules were obtained by PCR amplification from relevant genomic DNA unless
745 otherwise specified.

746

747 * The indicated fragments were obtained by PCR amplification from the plasmid of Scaf·CATGB
748 from our previous report [2]

749 ** The indicated fragments were obtained by PCR amplification from the plasmid of
750 Scaf·CATGB from our previous report [3]

751

752

753

Supplementary Figures

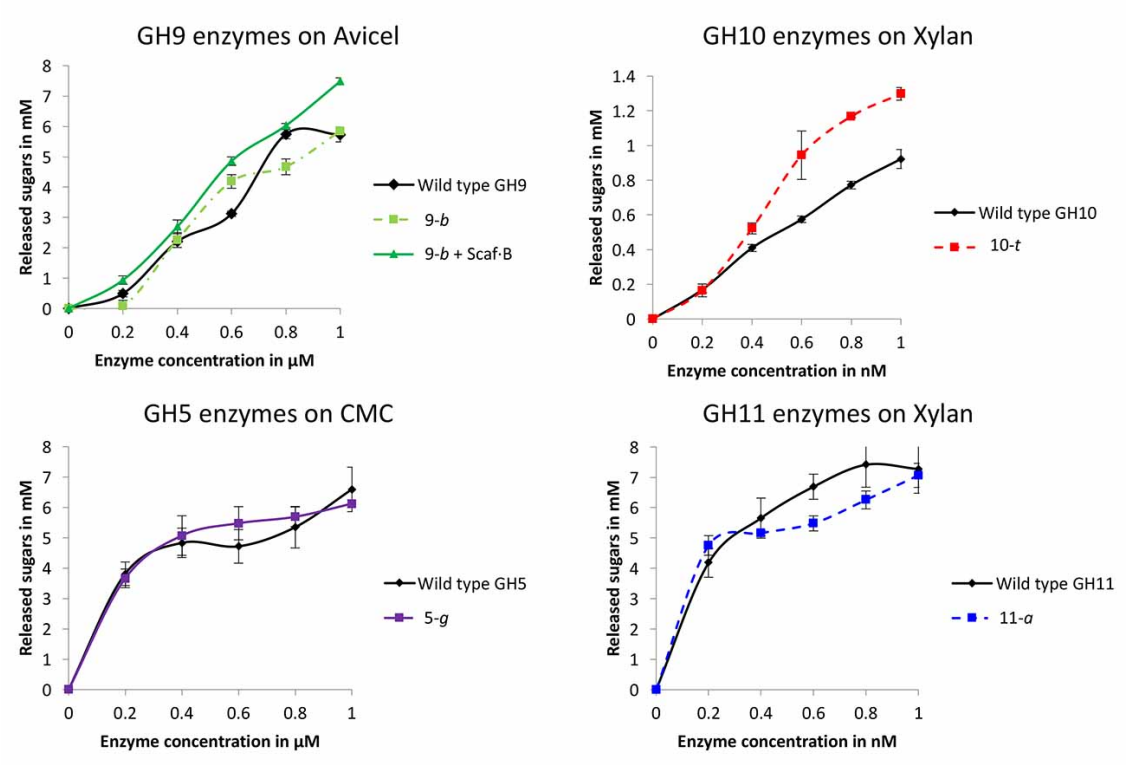

Fig S1. Hydrolytic activity profiles of the four recombinant *C. papyrosolvens* enzymes in comparison with the wild-type forms. The indicated enzymes were incubated 2 h at 37°C for xylan and CMC or 24 h for Avicel. Enzyme notation is given in Figure 1 of the article. Scaf·B refers to a monovalent scaffoldin, comprising the *C. thermocellum* scaffoldin-borne CBM3a and the *B. cellulosolvens* cohesin.

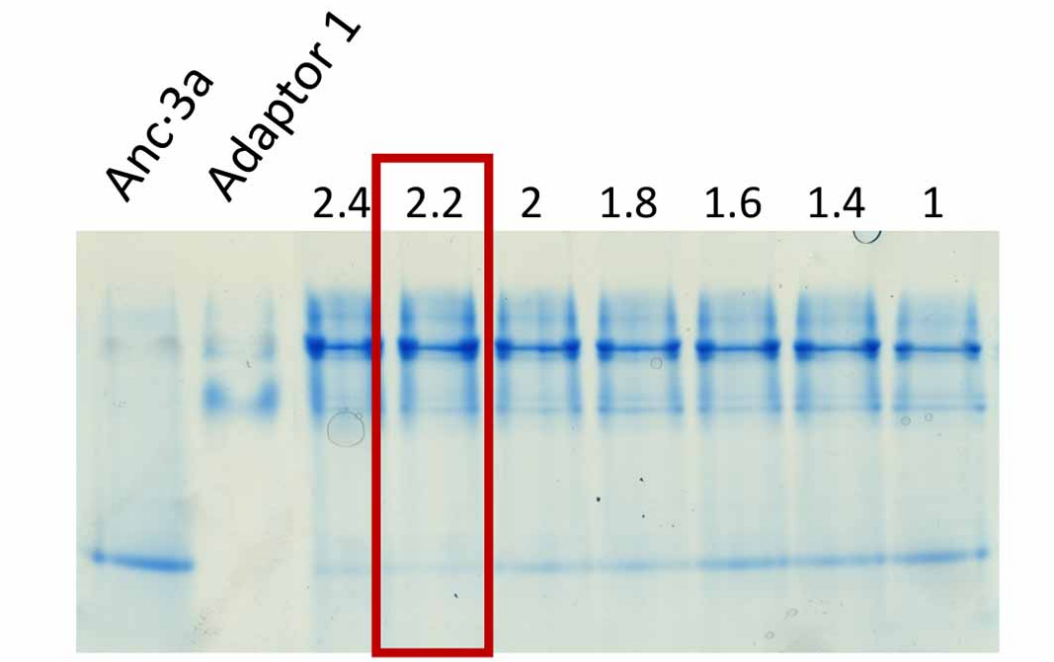

Fig. S2. Non-denaturating gel electrophoresis of the complex of pure recombinant Adaptor 1 with Anc·3a produced in *E. coli*. Lane 1: Anc·3a; Lane 2: Adaptor 1; Lanes 3 to 9: ratios of Adaptor 1/ Anc·3a (i.e. Lane 3, 2.4:1).

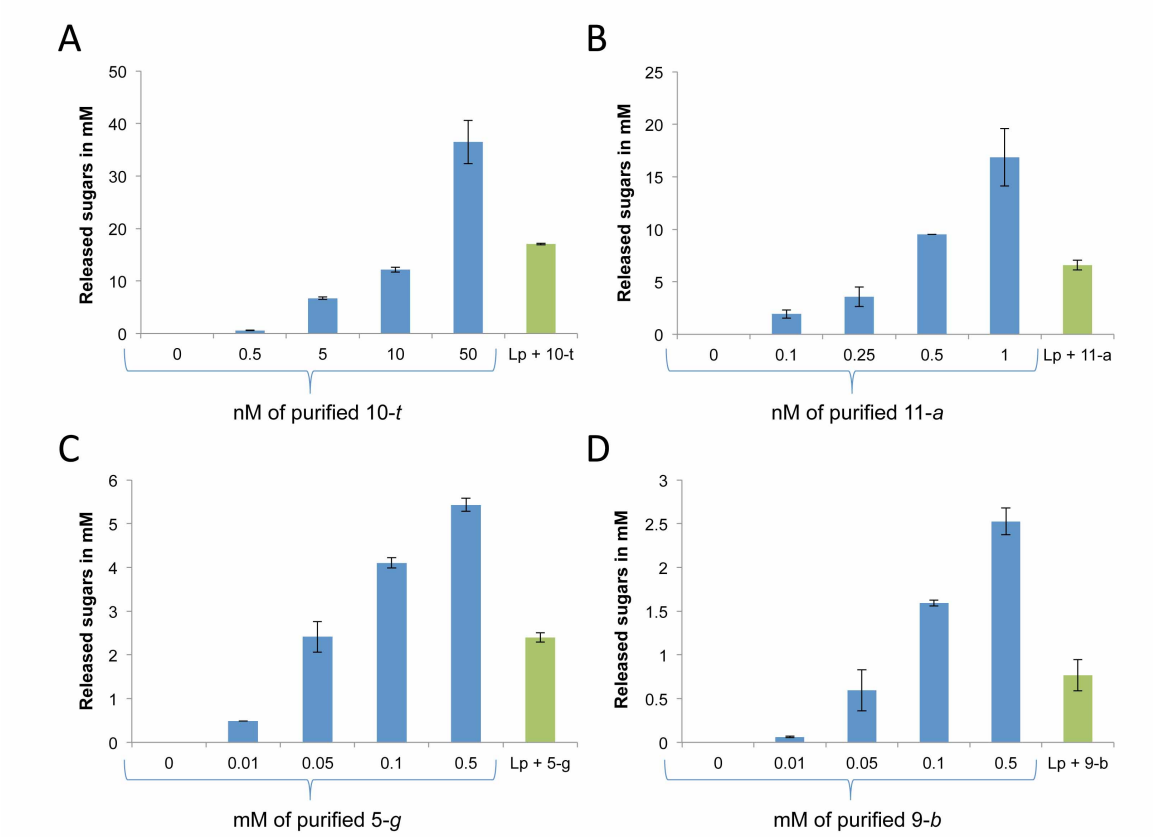

Fig. S3. Quantification of the secreted *L plantarum* enzymes by assessing comparative activity with known concentrations of pure recombinant proteins produced in *E. coli*. (A) and (B): enzymatic activity on xylan. Reactions were conducted with either increasing concentrations of purified *C. papyrosolvens* xylanases 10-*t* and 11-*a*, respectively, or with 30 µl of concentrated culture supernatant fluids, following a 2-h reaction period at 37°C. (C) and (D): enzymatic activity on carboxymethyl cellulose (CMC). Reactions were conducted with either increasing concentrations of purified *C. papyrosolvens* cellulases 5-*g* and 9-*b,* respectively, or with 30 µl of concentrated culture supernatant fluids following a 2-h reaction period at 37°C.

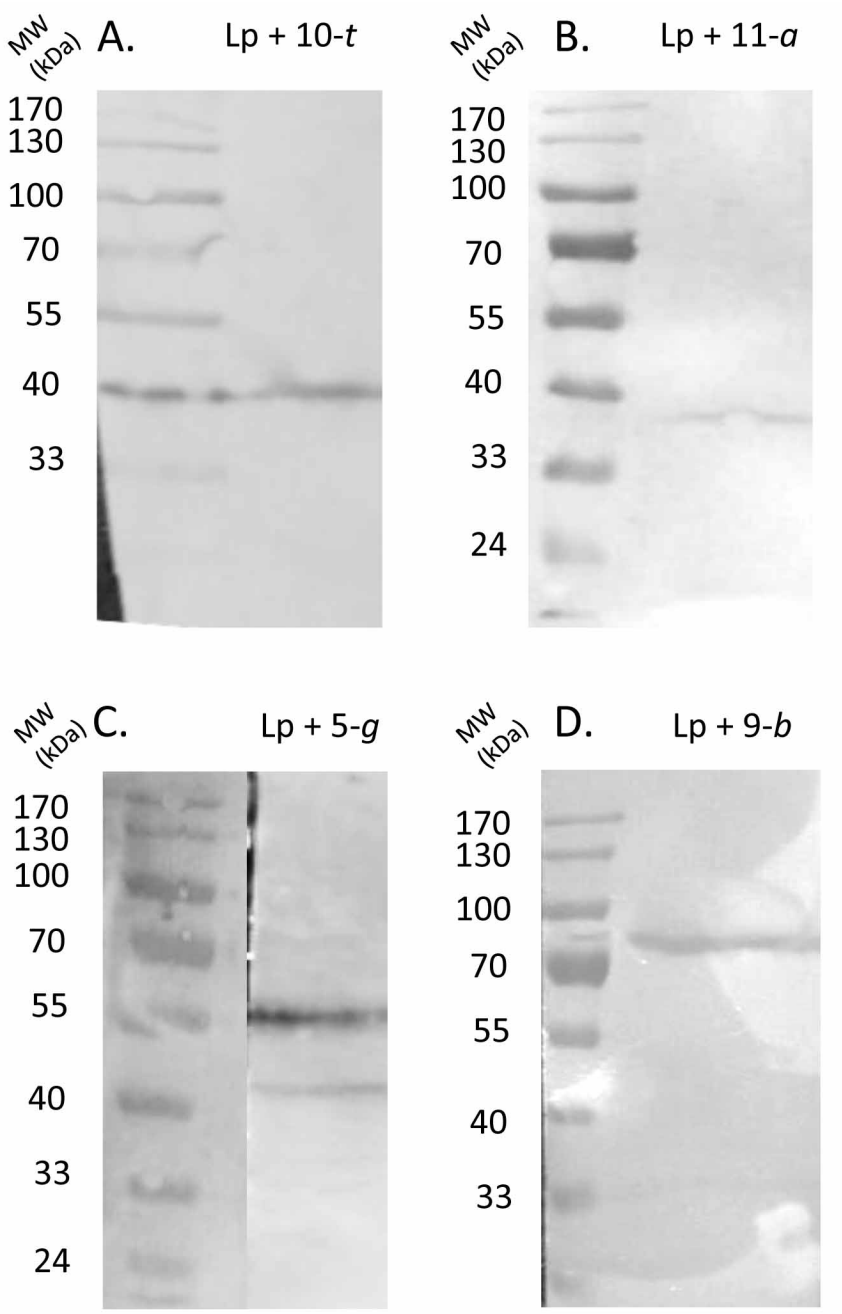

Fig. S4. Far-Western blot analysis (A, B, C and D) and Western blot analysis (E and F) of concentrated culture supernatant fluids from transformed lactobacilli versus respective pure recombinant proteins produced in *E. coli*. (A) Secreted 10-*t* (calculated mass 44.5 kDa), (B) secreted 11-*a* (calculated mass 33 kDa), (C) secreted 5-*g* (calculated mass 51.3 kDa), (D) secreted 9-*b* (calculated mass 77.6 kDa). **(**E) and (F): The lanes in the two panels (E) Adaptor·1 (calculated mass 79.3 kDa) and (F) Adaptor·2 (calculated mass 72.8 kDa) are as follows: Lanes 1-3: secreted Adaptor by *L. plantarum;* Lane 4-6: secreted fraction of wild-type *L. plantarum;* Lane 7-9: pure Adaptor produced by *E. coli*.

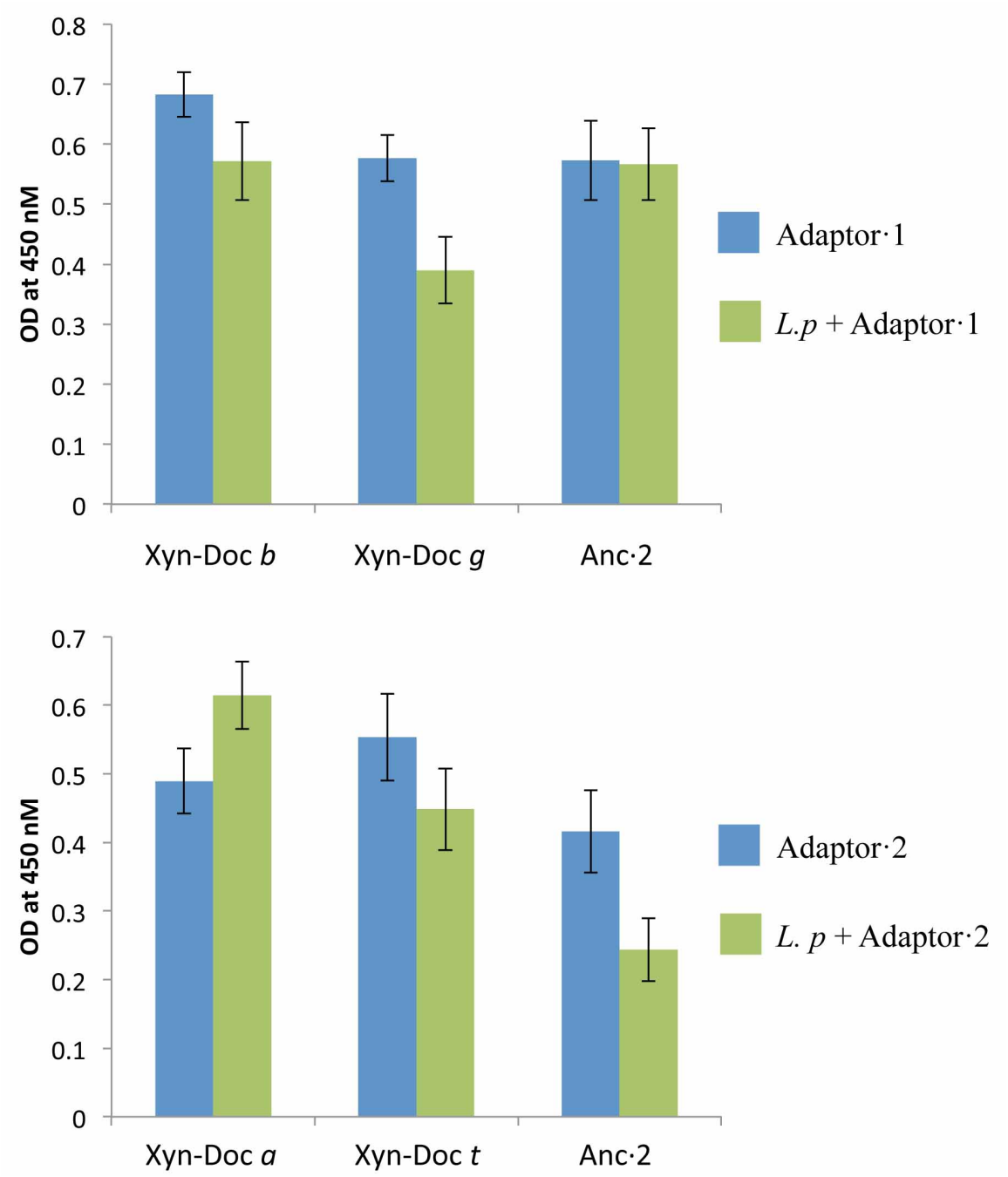

Fig. S5. ELISA-based binding assay of pure recombinant proteins produced in *E. coli* versus concentrated secreted proteins from transformed *L. plantarum*. Microtiter plates were coated with 1 μg/ml the purified proteins as specified in the X axis and subjected to interaction with either 100 ng/ml of pure adaptor scaffoldin (blue bars) or *L. plantarum* secreted adaptor scaffoldin (green bars). The primary antibody used here was elicited against the CBM of the scaffoldins (i.e., CBM3a of the *C. thermocellum* CipA scaffoldin). Concentrated secreted proteins from *L. plantarum* wild-type strain were used as a blank.

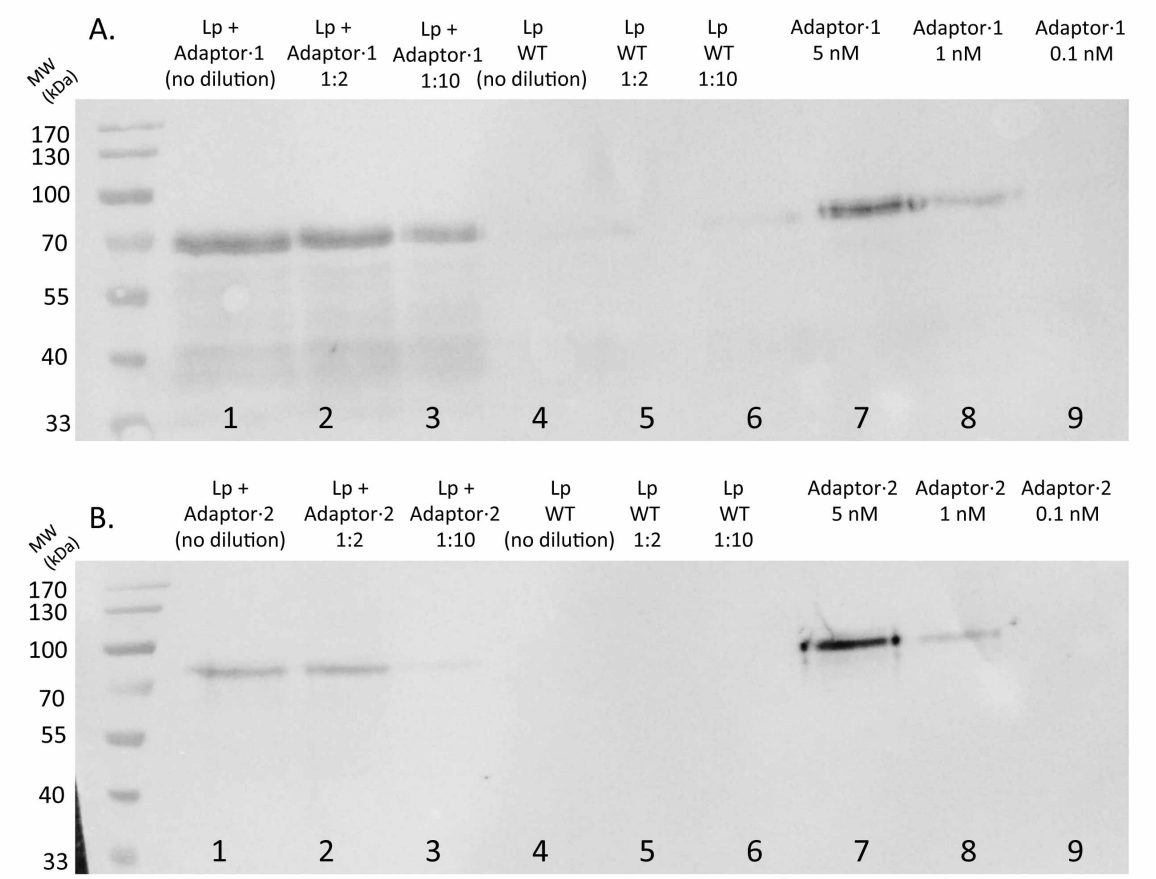

Fig. S6. ELISA binding assay of pure recombinant proteins produced in *E. coli* versus anchored proteins produced by *L. plantarum*. Microtiter plates were coated with 1 μg/ml of pure proteins produced in *E. coli* as specified in the x axis and subjected to interaction with either 100 ng/ml of pure chimaeric scaffoldin produced in *E. coli* (blue bars) or *L. plantarum* cells displaying the anchored scaffoldin (green bars). The primary antibody used for panels A, B, C and D was elicited against the type II cohesin from *C. thermocellum,* present on Anc·T_2F_3 (Anc 2), Anc·$2T_2F_3$ (Anc 3a), Anc·$T_2 2F_3$ (Anc 3b) and Anc·$2T_2 2F_3$ (Anc 4), where T_2 represents the type II *C. thermocellum* cohesin and F_3 represents the type III *R. flavefaciens* cohesin; for panel E, the primary antibody was elicited against the CBM of Anc·1. Washed bacterial cells (wild-type strain) served as a control.

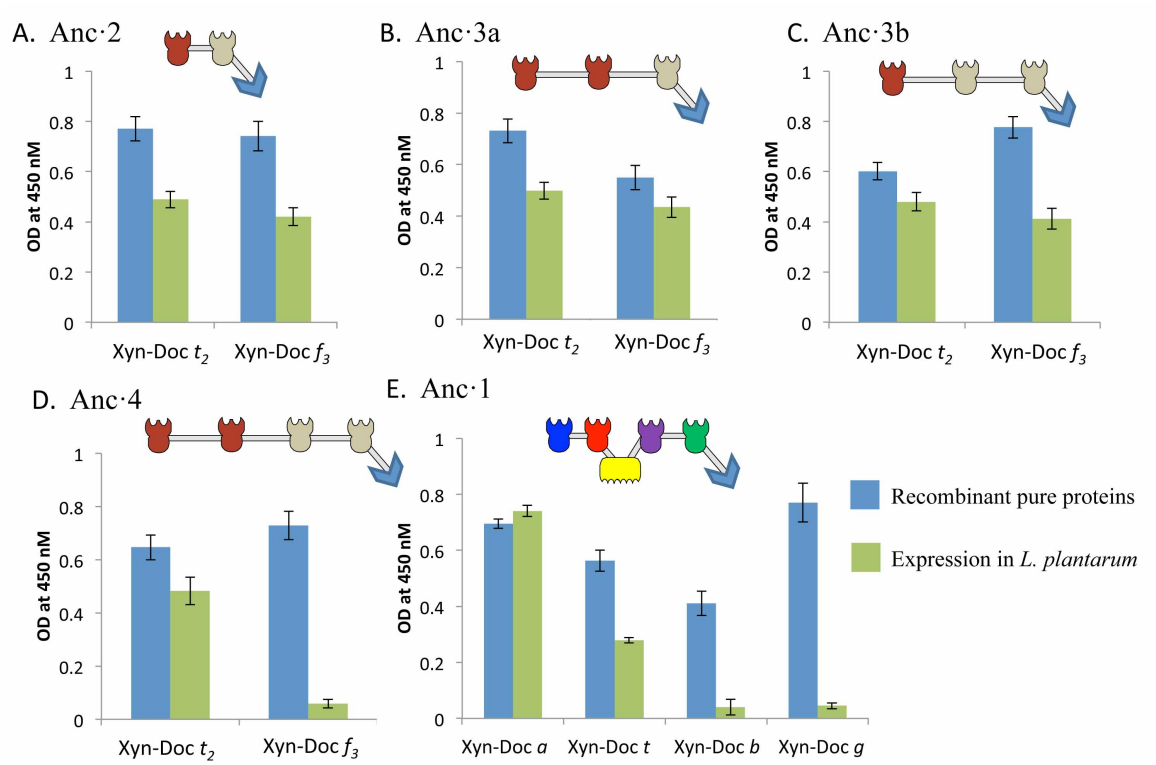

Fig.S7. Kinetics studies of hypochlorite-treated wheat straw hydrolysis up to 120-h incubation at 37°C by the different types of consortia. The composition of the consortia is as specified in Figure 3 panel B. Enzymatic activity is defined as total reducing sugars released (µM). Error bars show standard deviations.

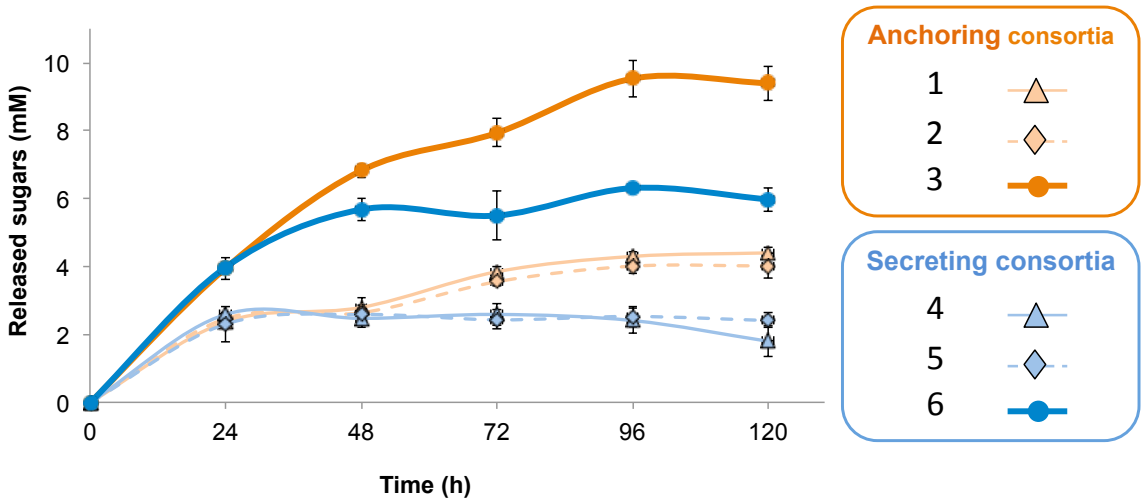

Fig. S8. Bacterial growth on incremental concentrations of sugars with chemically defined medium CDM supplemented with (A) cellobiose, and (B) glucose. Xylose and xylobiose as sole carbon sources could not sustain growth.